scientific reports

OPEN

The relationship between cloud distribution characteristics and meteorological elements over China

Yue Yang[1,2], HongKe Cai[2]✉ & Quan-Liang Chen[2]

The meteorological elements in the cloud background field influence and change with the cloud macro and micro characteristics, so it is of great significance to study the relationship between them. Using CALIOP Level 2 VFM products and ERA5 reanalysis data, this paper studies and analyzes the relationship between the distribution characteristics of different types and phases clouds and meteorological elements over China through statistical methods. The results show that: In the two-dimensional probability density function distribution of cloud occurrence probability and relative humidity-temperature, there are two significant high value regions, which can be divided into tropical clouds and temperate clouds. Further linear fitting of cloud and relative humidity-temperature two-dimensional probability density function shows that transparent altocumulus and altostratus show a similar linear trend, which indicates that the relationship between temperature and relative humidity is consistent in the background field with high frequency of mixed-phase clouds. Tropical and temperate cirrus may correspond to in-situ origin cirrus and liquid origin cirrus, respectively. Further analysis of the relationship between specific humidity and temperature in the cloud background field shows that with a high cloud occurrence probability, water vapor content was exponentially correlated with temperature. The ratio between the actual fitted water vapor and the saturated water vapor calculated by Tetens formula is defined as the water vapor content saturability in the cloud background field. It is found that the water vapor content saturability in the cloud background field increases with the decrease of temperature, and this trend is more obvious in cirrus.

Keywords CALIOP, Cloud types, Cloud phases, Meteorological elements

Any change in cloud distribution characteristics may cause changes in meteorological elements of its background field, and likewise, changes in meteorological elements can in turn cause adjustments in cloud distribution characteristics[1–3]. Previous studies have shown that meteorological elements such as temperature and humidity are key influencing factors in cloud thermal dynamic processes[4,5] and micro physical processes[6]. Cai et al.[7] found that the distribution boundary of ice clouds and water clouds is very close to the isotherm of −14℃ at the height of 3–7 km, and this relationship may be related to the mechanism by which water clouds transform into mixed-phase clouds with the assistance of ice nucleating particles (INPs). Relative humidity (RH) is an extremely important factor in cloud parameterization. Many meteorological elements (such as vertical velocity) and aerosols affect the distribution characteristics of clouds by influencing RH[8]. In addition, RH is also closely related to the ice supersaturation process during cloud formation[9]. D 'Alessandro et al.[10] compared the cloud phases and RH distribution of −67 ℃ to 0 ℃ over the Southern Ocean in the summer of the Southern Hemisphere, and compared it with the global climate simulation, and found that the deviation between the RH of the ice cloud and the liquid saturability was as high as 20%−40% at −20 ℃ to 0 ℃. This indicates that for low liquid mass fraction (< 0.1), the assumption of liquid saturability model for coexistence of ice and liquid is not accurate. Therefore, the study of meteorological elements in the cloud background field is conducive to improving the parameterization scheme of global atmospheric models to simulate the physical process of cloud

[1]Xindu District Meteorological Bureau, Chengdu 610500, China. [2]Climate Change and Resource Utilization in Complex Terrain Regions Key Laboratory of Sichuan Province, Chengdu Plain Urban Meteorology and Environment Observation and Research Station of Sichuan Province, Sichuan Provincial Engineering Research Center for Meteorological Disaster Prediction and Early Warning, School of Atmospheric Sciences, Chengdu University of Information Technology, Chengdu 610225, China. ✉email: caihk@cuit.edu.cn

formation, so as to comprehensively evaluate the characteristics of clouds and their impacts on climate in global climate and weather forecasting models.

Schoeberl et al.[11] studied the relationship between the cloud distribution of tropical tropopause layer (TTL) and the ice-related high relative humidity (RHi), and found that high (>80%) RHi region generally existed in TTL, and the region with the highest RHi was consistent with the extensive cirrus cloud distribution. By analyzing the statistical relationship between cirrus micro-physics and large-scale meteorology, Muhlbauer et al.[12] found that almost half of cirrus occurrence near observation sites can be explained by three different weather conditions, namely, upper ridges, mid-latitude cyclones with frontal systems, and subtropical currents. The probability density function (PDF) of cirrus micro-physical properties, such as particle size distribution, ice number concentration, and ice water content, show significant differences across weather systems. Klein and Hartmann[13] found that there was a strong correlation between low cloud cover over the ocean and the potential temperature difference between 700 hPa and sea level, that is, low tropospheric stability. Wood and Bretherton[14] further proved that there was a positive correlation between liquid stratospheric cloud cover and low tropospheric stability. The matter-backscattering ratio of cirrus is negatively correlated with temperature[15–18] and the shape ratio of particles in cirrus is also strongly correlated with temperature, in which the depolarization rate increases with the decrease of temperature[19,20]. CALIOP Level 2 VFM products, which classifies clouds and aerosols through scene classification algorithms (SCA), provides cloud climate data with wider coverage and higher resolution[7]. VFM products can be used to further study the relationship between the distribution characteristics of different types and phases clouds and meteorological elements. Therefore, this paper uses ERA5 data as the background field of meteorological elements and combined with CALIOP VFM data to study the relationship between cloud distribution characteristics and meteorological elements.

This paper is organized as follows: Section. 2 presents the satellite observation and reanalysis data used to analyze the relationship between cloud distribution characteristics and meteorological elements. Section 3 describes the relationship between cloud distribution characteristics of different types and phases and RH. Section 4 describes the relationship between cloud distribution characteristics of different types and phases and specific humidity (SH). Section 5 summarizes and looks forward to the full paper.

Data and method
Data
Cloud types in VFM products are divided into eight categories[7]: low overcast (transparent), low overcast (opaque), transition stratocumulus, low broken cumulus (transparent), altocumulus (transparent), altostratus (opaque), cirrus (transparent) and deep convective (opaque). The sample selected in this paper is a laser beam that can penetrate clouds to the ground, and the research only targets clouds with optical thickness ranging from 0.02 to 3[7]. Some deep convective clouds cannot be detected in the vertical direction by laser radar owing to their large thickness. Therefore, they are not included in the statistical analysis in this paper. In addition, CALIOP L2-VFM provides corresponding quality assessment. According to the cloud-aerosol recognition algorithm, the identification results are marked with confidence, which are classified into four categories: high, medium, low and untrustworthy. Among them, over 90% are highly trustworthy, and 90% are calculated by the CAD data recognition algorithm in VFM products[21]. The data used in this paper is the highly trustworthy part of the VFM products.

Level 2 VFM vertical mask products from CALIPSO and ERA5 (ECMWF Reanalysis v5) meteorological element data from June 2006 to June 2020 are combined in this study. The relationship between the distribution characteristics of different types and different phases of clouds and meteorological elements in China and surrounding areas (0–55°N,70–140°E) was analyzed.

Research and method
In this paper, China and its surrounding areas (0–55°N, 70–140°E) are selected as the research area (Fig. 1). The red line in the figure is the outline of the Qinghai-Tibet Plateau, and the contour recognition is based on the 3000 m contour line of ETOPO5 Global Surface Relief[22,23].

The horizontal resolution of the VFM product used in this paper is 333 m, and the 1°×1° products can obtain quite a lot of samples in the grid: the average number of observed profiles after 1°×1° gridding is above 123,000, and the average number of observed tracks is above 440[7]. Therefore, it is subjected to quality control and gridding, that is, by dividing 1°×1° grids, scattered particles of different heights detected by each profile in each grid are taken as samples. Then, the grid data of 1°×1° were statistically analyzed to form a cloud sample data set of 1°×1° for 15 years, and then the spatial-temporal characteristics of various types of clouds were statistically analyzed. For the ERA5 reanalysis data with a resolution of 0.25°×0.25°, this paper uses the nearest neighbor interpolation method to match the 0.25°×0.25° reanalysis data with the horizontal resolution of 333 m satellite data. The most recent 0.25° reanalysis data is used in the VFM products to form cloud and meteorological element matching samples in the cloud background field, which are used to analyze the relationship between the cloud and meteorological elements, that is, the statistical analysis in Sects. 3-4.

Results
The relationship between relative humidity and cloud types distribution characteristics
Combining RH and temperature (Fig. 2), the probability of cloud occurrence presents two significant high value regions along with the change trend of the two meteorological elements. When the temperature is colder than 0 ℃, low clouds mainly occur under conditions of low temperature and high RH. When the temperature is warmer than 10 ℃, clouds mainly occur under conditions of high temperature and high RH (Fig. 2a-d). For transparent altocumulus (Ac, tra) and opaque altostratus (As, op) (Fig. 2e and f), when the temperature
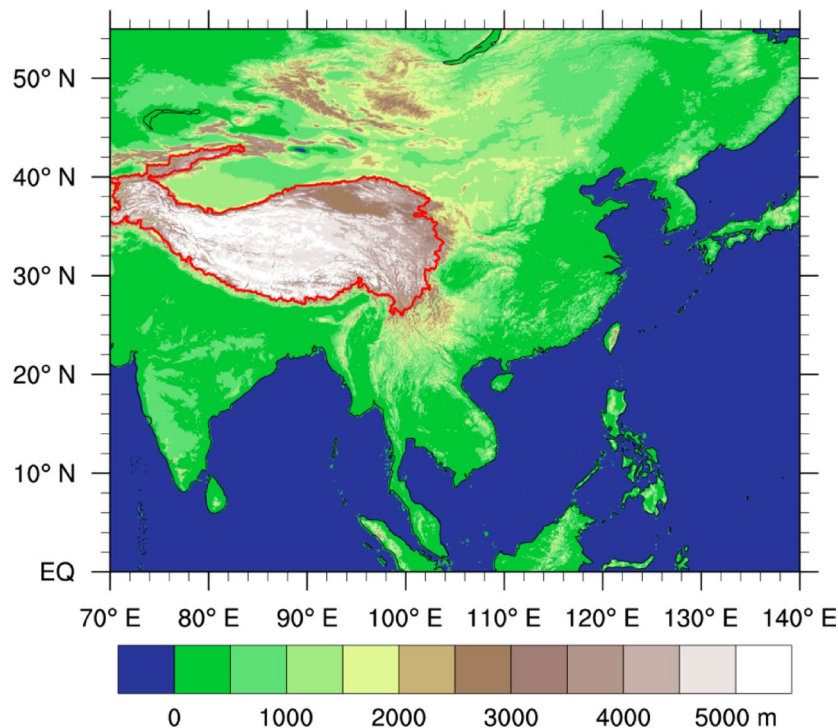
Fig. 1. Terrain of the study area (This map was created by NCAR Command Language Version 6.5.0 (download the software at https://www.ncl.ucar.edu/Download/). Terrain data is derived from the Shuttle Radar Topography Mission (SRTM), data download https://srtm.csi.cgiar.org/SELECTION/inputCoord.asp).
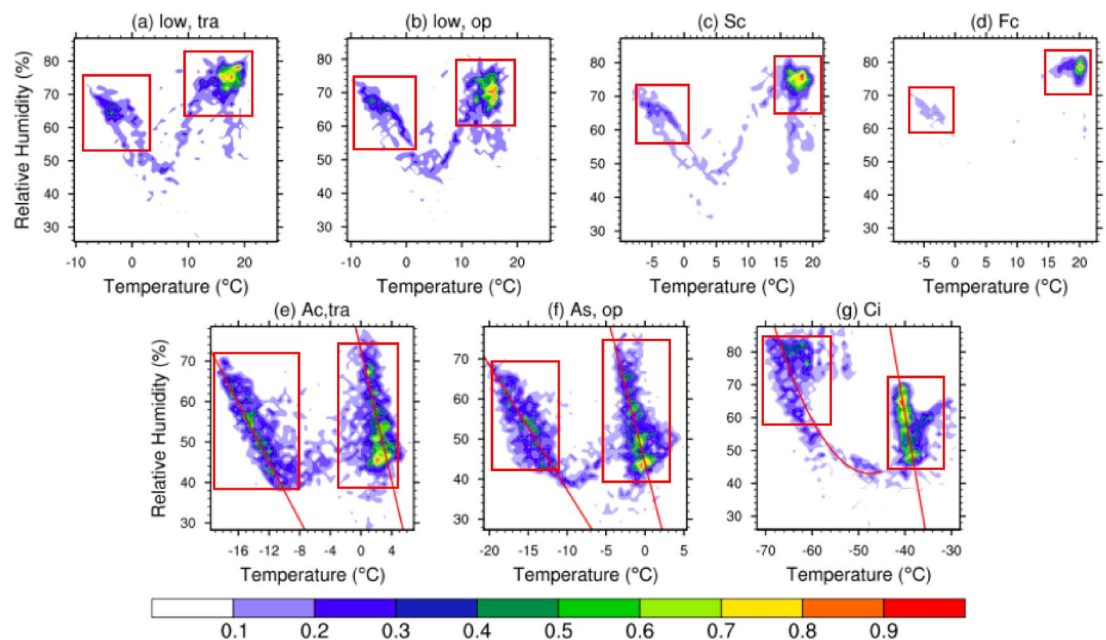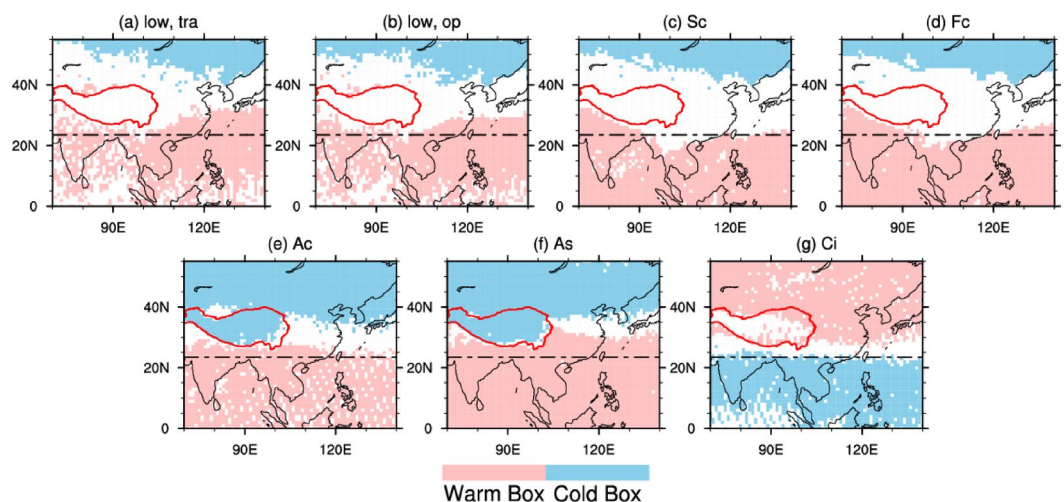

Fig. 2. The PDF distribution of RH and cloud temperature: **(a)** low overcast (transparent), **(b)** low overcast (opaque), **(c)** stratocumulus, **(d)** low broken cumulus (transparent), **(e)** altocumulus (transparent), **(f)** altostratus (opaque) and **(g)** cirrus.

is colder than $-10\ ^{\circ}\text{C}$, the clouds mainly occur under conditions of low temperature and high RH. When the temperature is warmer than $0\ ^{\circ}\text{C}$, the probability of cloud appearance increases as the RH decreases. Moreover, the probability of occurrence of the two types of cloud shows a significant linear trend. Therefore, the linear fitting of the two-dimensional PDF of RH and temperature of Ac and As was further carried out (Fig. 2e and

f), and it was found that the cold temperature and high frequency region of Ac could be well fitted to a straight line with a slope −3.61 and an intercept 1.75. The warm temperature and high frequency region can better fit a straight line with a slope of −8.05 and an intercept of 72.64. As also shows a similar linear trend, which indicates that the RH and temperature present a linear change in the background field with high frequency of the two kinds of mixed-phase clouds, Ac and As. The slope of linear change at different temperatures is close but the intercept is different, that is, the relationship between temperature and RH is consistent but RH is different. The occurrence probability of cirrus is also divided into two parts by temperature, in which it mainly appears at −40 ℃ and increases with the increase of RH. The secondary part appears at −60 ℃ to −70 ℃, and the probability of occurrence also increases with the increase of RH. Further, the two-dimensional PDF of RH and temperature of cirrus is linearly fitted, and it is found that the cold temperature high frequency region of cirrus could be well fitted to a curve, and the warm temperature high frequency region could be well fitted to a straight line, indicating that under cold temperature conditions, in the background field with high frequency of cirrus, the RH and temperature show corresponding curve changes. Under warm temperature conditions, in the background field with high cirrus occurrence frequency, the RH and temperature show a linear change. Such different trends may be related to the differences in the formation mechanisms of the two types of cirrus.

In view of the distribution characteristics of double high-value regions shown by two-dimensional PDF of RH and temperature of cloud types, clouds of the same type conforming to the characteristics of the two high-value regions are defined as cold-temperature clouds (i.e., the left box of Fig. 2) and warm-temperature clouds (i.e., the right box of Fig. 2) respectively according to the temperature differences, and the horizontal distribution characteristics of the two are further analyzed. It is found that in Fig. 3(a) - (f), except cirrus, the cold clouds in all types of clouds are mainly distributed in the north of 40 °N, the mixed-phase clouds extend southward to the Qinghai-Tibet Plateau, and can be defined as temperate clouds, while the warm clouds are mainly distributed in the low latitude area, and the northern boundary is near the Tropic of Cancer, and can be defined as tropical clouds. For cirrus, it shows the opposite distribution characteristics, cold cirrus is mainly distributed in the low latitude region, and the northern boundary is also near the Tropic of Cancer, so it is defined as tropical cirrus, while warm cirrus is mainly distributed in the temperate region. Tropical cirrus and temperate cirrus may correspond to two types of cirrus with different formation mechanisms and micro-physical properties: in-situ origin cirrus and liquid origin cirrus[24]. He et al.[25] indicated that liquid origin cirrus is mostly formed by heterogeneous nucleation, while in-situ origin cirrus is mostly formed by homogeneous nucleation[26]. Cai et al.[7] found that cirrus at middle and high latitudes are more likely to be formed by heterogeneous nucleation, while cirrus at low latitudes are more likely to be formed by homogeneous nucleation. The horizontal distribution difference of cirrus in Fig. 3(g) also corresponds to such a relationship, that is, cirrus in temperate regions correspond to liquid origin cirrus formed mainly by heterogeneous nucleation. Cirrus in the tropics correspond to in-situ origin cirrus formed primarily by homogeneous nucleation. In the two-dimensional PDF distribution of temperature and RH (Fig. 3g), tropical cirrus exhibit a characteristic of high RH, further confirming that they might correspond to in-situ origin cirrus directly formed in the form of ice under low-temperature and high-humidity conditions. Temperate cirrus exhibit the characteristic of low RH, further confirming that they correspond to liquid origin cirrus formed by the freezing of liquid droplets in the cloud under conditions of high temperature and low humidity. The different formation mechanisms of these two types of cirrus may be the reason why the RH and temperature in cirrus background field show curve and linear trend respectively under cold temperature and high temperature conditions. Krämer et al.[27] also drew a similar conclusion. They found that the RH in cirrus shows typical latitude differences, with the RH in cirrus being higher in tropical regions and lower in temperate regions. The difference between temperate and tropical distribution of this cloud type indicates that temperature rather than RH is the main meteorological factor associated with the distribution

Fig. 3. is the same as Fig. 2, but shows the horizontal distribution of clouds in the PDFs high value area of RH and temperature (the black dashed line is the Tropic of Cancer 23.5°N, the red solid line is the terrain of the Qinghai-Tibet Plateau).

characteristics of the cloud type. Moreover, the background field temperature is mainly caused by latitude differences, and the relationship between RH and cloud distribution characteristics may be due to temperature changes.

The relationship between relative humidity and cloud phases distribution characteristics
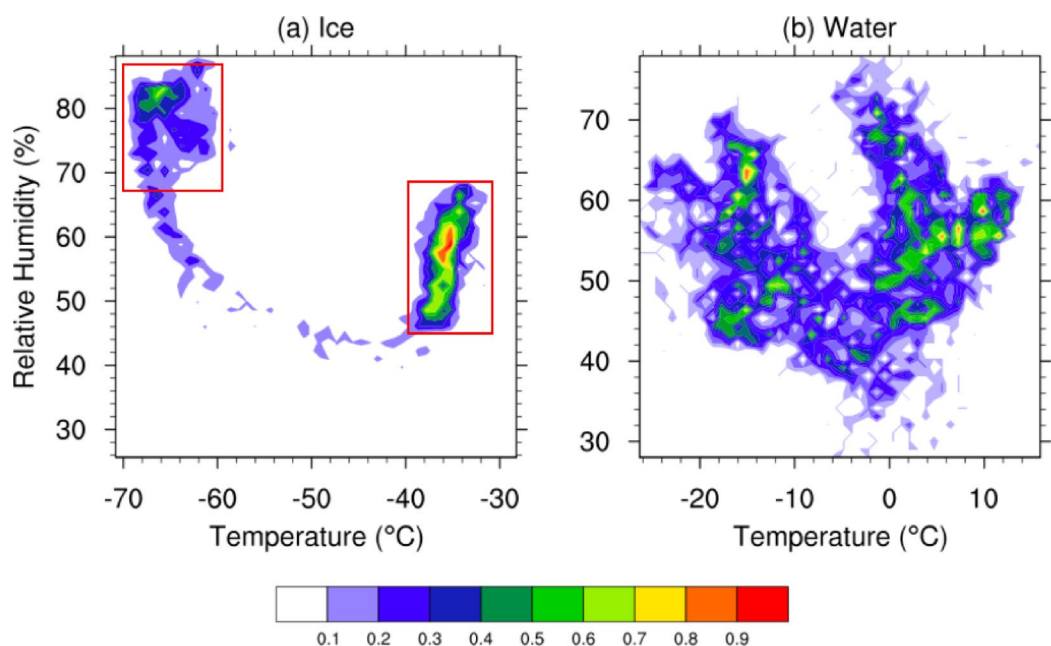
As shown in Fig. 4, the PDF distribution of RH and temperature corresponding to ice cloud is similar to cirrus, which is also mainly divided into two parts by temperature, in which the temperature mainly occurs at −40 ℃ to −30 ℃, and increases with the increase of RH. The secondary part appears at −60 ℃ to −70 ℃, and the probability of occurrence also increases with the increase of RH. Combining the two high-value regions of cloud occurrence probability, the RH of ice cloud increases with the decrease of temperature, which is consistent with the conclusion reached by Alexei and George[28]. The trend of water cloud occurrence probability with the change of the two meteorological elements does not show obvious characteristics of the two high-value regions, but it also shows roughly two types of trend. When the temperature is colder than 0 ℃, the colder the temperature and the higher the RH, the greater the probability of cloud occurrence. When the temperature is warmer than 0 ℃, the warmer the temperature and RH, the greater the probability of cloud occurrence.

In view of the distribution characteristics of the double high-value region shown by two-dimensional PDF of the RH and temperature of the ice cloud, the same type of clouds conforming to the characteristics of the two high-value regions are divided into cold ice clouds (i.e., the left box of Fig. 4) and warm ice clouds (i.e., the right box of Fig. 4) according to the temperature difference, and the horizontal distribution characteristics of the two are further analyzed (Fig. 5). The results are consistent with the distribution characteristics of cloud types. Cold ice clouds are mainly distributed in temperate areas, with the southern boundary around 30 °N, while warm ice clouds are mainly distributed in tropical areas, and the northern boundary is also near the Tropic of Cancer. Based on the cloud height data in the VFM products, the ice cloud height in China and its surrounding areas was calculated. It was found that in areas south of 35°N, the ice cloud height is generally above 9 km. Zhang et al.[29] found that clouds with cloud top height below 9 km are more closely related to topography, while the cloud above 9 km has little relationship with topography, so the ice cloud is less affected by the topography of the Qinghai-Tibet Plateau, resulting in the southern boundary of the ice cloud region is relatively flat. This difference in latitude distribution is more obvious than that of cloud types, and the 25 °N-30 °N latitude zone is a significant dividing zone between temperate and tropical ice cloud coverage.

The relationship between specific humidity and distribution characteristics of cloud types

RH is a physical quantity calculated from the actual water vapor pressure and saturated water vapor pressure, which is related to temperature. Therefore, the cloud distribution characteristics displayed are also greatly affected by temperature, and the relationship between humidity and cloud climatology characteristics cannot be fully expressed. In order to reveal the relationship between water vapor content in background field and cloud distribution characteristics, the variable SH is introduced, and the SH corresponding to cloud types is analyzed by PDF.

Comparing SH with temperature, it can be seen from two-dimensional PDF distribution (Fig. 6) that as the temperature decreases, the water vapor content in the background field where all kinds of clouds are located

Fig. 4. is the PDF distribution of RH and cloud temperature in the cloud background field: **(a)** ice cloud, **(b)** water cloud.
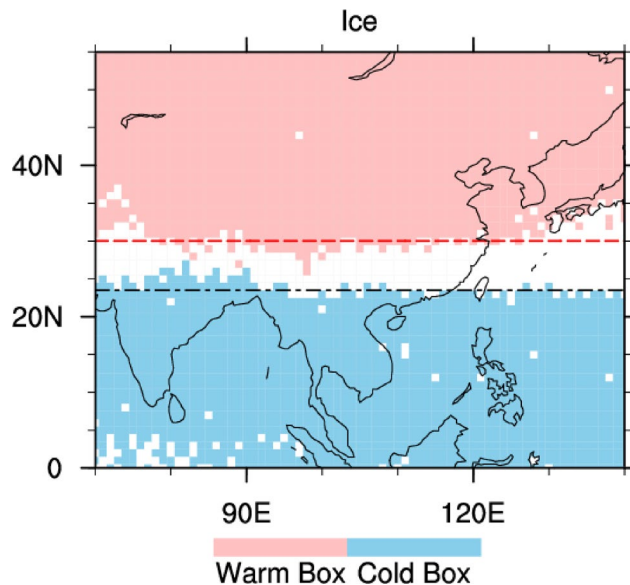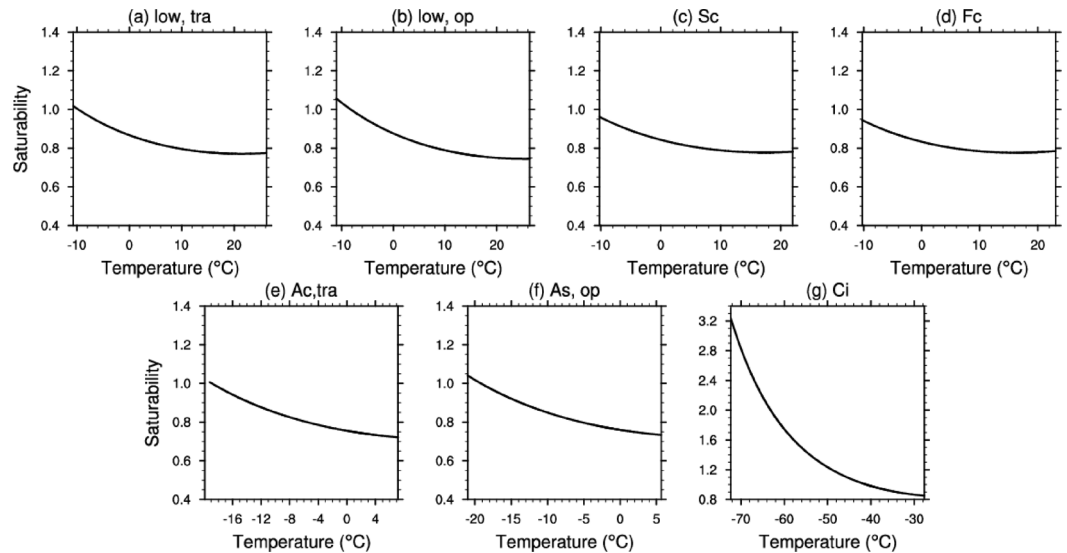
Fig. 5. is the same as Fig. 4 but shows the horizontal distribution of ice clouds in the PDF high value area of RH and temperature (black dotted line is the Tropic of Cancer 23.5°N, red dotted line is 30°N).
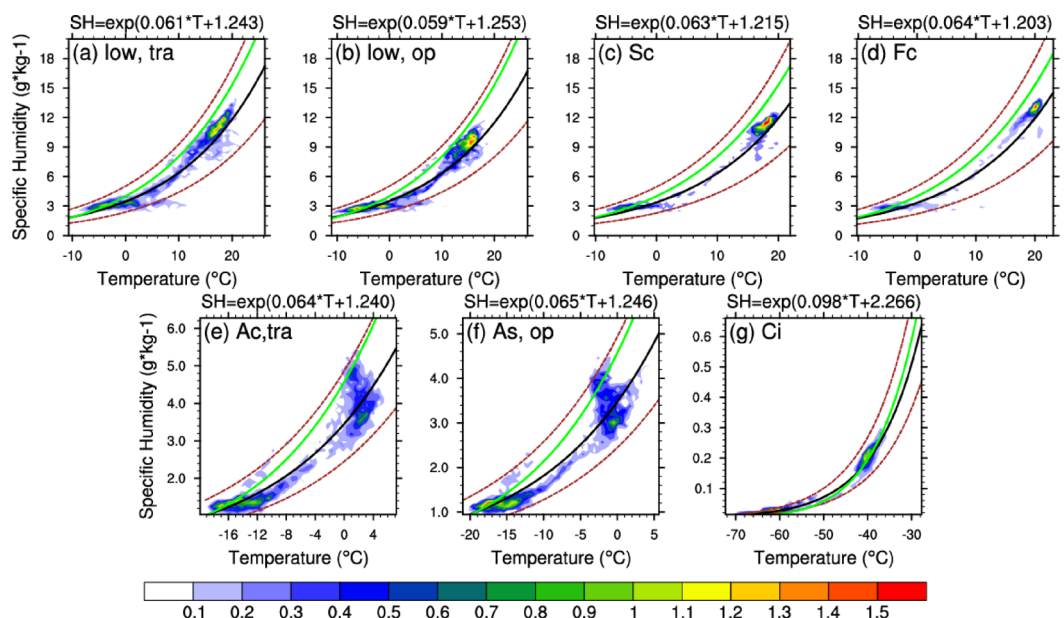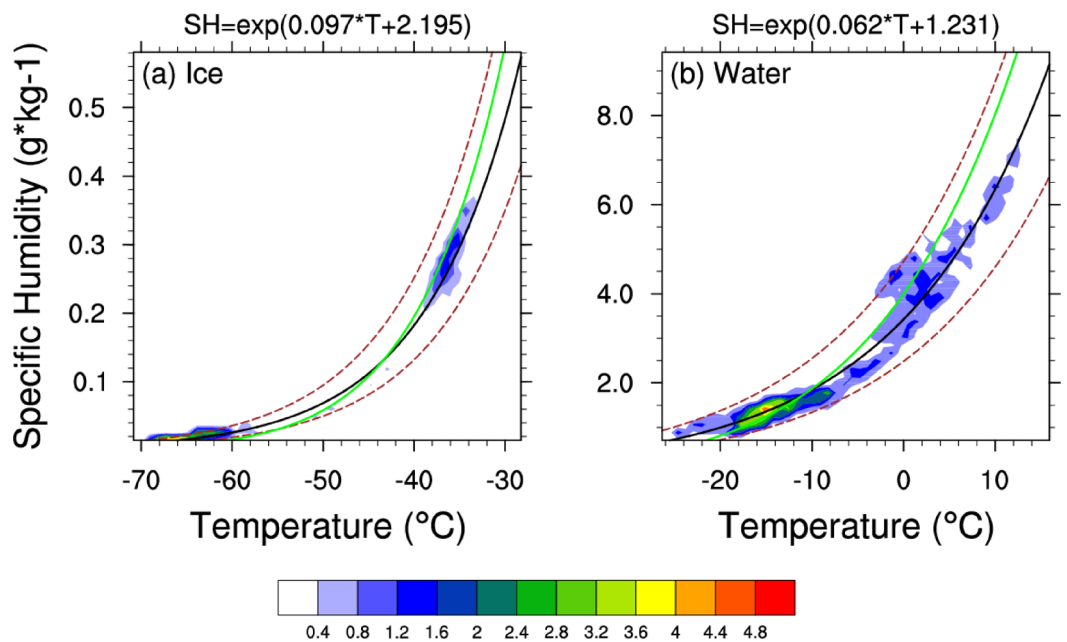

Fig. 6. is the same as Fig. 2, but shows the PDF distribution and exponential fitting of specific humidity and temperature in the cloud background field (the filling color is a two-dimensional PDF of SH and temperature in the background field, the black solid line is the actual fitting line, the brown dotted line is the 95% prediction interval, and the green solid line is the Tetens saturated water vapor pressure formula curve).

decreases. For clouds at different levels, the SH in the background field of low clouds is mainly between 2 and 14 $g \cdot kg^{-1}$, and the probability of cloud occurrence is higher under warm temperature and high SH conditions, while the SH of medium cloud is between 1 and 6 $g \cdot kg^{-1}$, and the probability of cloud occurrence is higher under cold temperature and low SH conditions. For high clouds such as cirrus, the water vapor content is obviously less than other clouds, and it is more in the background field condition where the SH is less than 0.1 $g \cdot kg^{-1}$. Figure 6 also reflects the positive correlation between water vapor content and temperature change for different types of clouds. In order to reveal the positive correlation between SH and temperature in the background field where the cloud distribution is located, this distribution is further fitted. The fitting results pass the 99% significance test, and all samples are within the 95% prediction interval. As shown in Fig. 6, in the background field of all types of clouds, water vapor content and temperature shows an obvious exponential correlation. In addition, Tetens saturated water vapor pressure formula[30] is introduced and combined with the

Fig. 7. is the same as Fig. 2, but shows the change of water vapor content saturability with temperature in the cloud background field.


Fig. 8. is the same as Fig. 4, but it is the fitting of the PDF distribution index of specific humidity and temperature in the ice cloud background field (the filling color is the two-dimensional PDF of specific humidity and temperature in the background field, the black solid line is the actual fitting line, the brown dotted line is the 95% prediction interval, and the green solid line is the Tetens saturability water vapor pressure formula curve).

actual fitting curve, it can be found that for all types of clouds, the water vapor content in the background field is basically unsaturated, and the water vapor content in the cirrus background field is close to saturability.

The ratio between the actual fitted water vapor and the saturated water vapor calculated by Tetens formula is defined as the water vapor content saturability in the cloud background field. As shown in Fig. 7, the water vapor content saturability in the cloud background field increases with the decrease of temperature, and this trend is more obvious in cirrus.

The relationship between specific humidity and distribution characteristics of cloud phases

For different cloud phases, as shown in Fig. 8, the water vapor content in the background field of ice clouds is significantly less than that of water clouds. And ice clouds are mainly distributed in the background field with
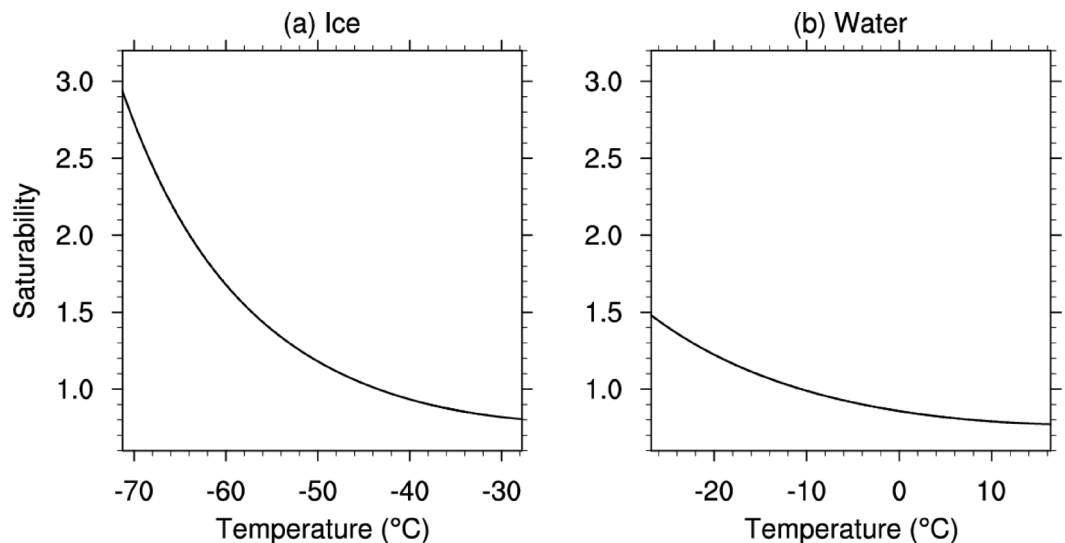
Fig. 9. is the same as Fig. 4, but shows the change of water vapor content saturability with temperature in the cloud background field.

water vapor content much less than $0.1 \ \mathrm{g} \cdot \mathrm{kg}^{-1}$. The background field of different cloud phases also shows that the water vapor content has a certain relationship with temperature. In order to reveal the positive correlation between SH and temperature in the background field where the different phases of clouds distribution are located, and further fit the distribution, it can be found that the water vapor content and temperature present obvious exponential changes at the location of cloud distribution, indicating that the water vapor content is exponentially correlated with temperature in the background field where clouds can be formed. And this exponential change relationship is particularly obvious in water clouds. By comparing the Tetens formula with the actual fitting curve, it can be found that for ice clouds, the water vapor content in the background field gradually becomes saturated with the decrease of temperature, while the water vapor in the background field is saturated below $-10℃$ and unsaturated above $-10℃$.

The saturability of water vapor content in the background field of different phase clouds increases with the decrease of temperature (Fig. 9). The fluctuation range of water vapor saturability of ice clouds is between 0.8 and 2.9, indicating that a part of ice clouds is still unsaturated, and the proportion of unsaturated ice clouds increases with the increase of ice cloud temperature. This is consistent with the conclusion once obtained by Alexei and George (2006). The fluctuation range of water vapor saturability of water cloud is between 0.8 and 1.5. The minimum water vapor saturability of water cloud is close to that of ice cloud, but the maximum water vapor saturability is significantly different.

Conclusion
In order to more accurately understand the relationship between cloud climate characteristics and meteorological elements in China and its surrounding areas, this paper uses CALIOP VFM, a high-resolution data product that can uniformly classify cloud types and cloud phases, and combines ERA5 reanalysis data to study the relationship between cloud types and cloud phases distribution characteristics and meteorological elements in China and surrounding areas during the 15-year period from June 2006 to June 2020. The main conclusions are as follows:

(1) Clouds occurrence probability presents two significant high value regions with the changing trend of RH and temperature. Clouds are mainly divided into tropical clouds and temperate clouds in the high value region of cloud occurrence probability, and the northern limit of tropical cloud coverage is near the Tropic of Cancer. Tropical cirrus clouds show high RH, which may correspond to the in-situ origin cirrus formed directly in the form of ice under low temperature and high humidity conditions, while temperate cirrus clouds show low RH characteristics, which corresponds to the liquid origin cirrus formed by freezing droplets in the cloud under high temperature and low humidity conditions. The relationship between RH and cloud distribution characteristics is mainly based on the change of temperature, and the temperature change mainly comes from the difference of latitude.

(2) In the background field with a high probability of cloud occurrence, the trend of specific humidity and temperature presents a positive correlation. The background field of low cloud is more inclined to high temperature and high humidity, while the background field of medium and high cloud is mainly low temperature and low humidity. Further analysis shows that water vapor content is exponentially correlated with temperature, and this correlation is particularly obvious in water clouds. The ratio of the actual fitted water vapor to the Tetens saturated water vapor was defined as the water vapor saturability in the cloud background field. It was found that the water vapor saturability in the cloud background field increased with the decrease of temperature, and this trend was more obvious in cirrus.

Data availability

The datasets analyzed during the current study are available in the CALIPSO official website [https://www-calipso.larc.nasa.gov/] and Climate Data Store [https://cds.climate.copernicus.eu/].

References

1. Wetherald, R. T. & Manabe, S. Cloud feedback processes in a general circulation model. *J. Atmos. Sci.* **45** (8), 1397–1416 (1988).
2. Li, Z. & Le Treut, H. Cloud-radiation feedbacks in a general circulation model and their dependence on cloud modelling assumptions. *Clim. Dynam.* **7**, 133–139 (1992).
3. Pan, H., Wang, M., Kumar, K. R., Zhang, J. & Lu, M. : A decadal global climatology of ice cloud fraction with their microphysical and optical properties inferred from the CALIPSO and reanalysis data. *Remote Sens.* 12(22), 3795 (2020). (2020).
4. Wood, R. & Bretherton, C. S. On the relationship between stratiform low cloud cover and lower-tropospheric stability. *J. Clim.* **19** (24), 6425–6432 (2006).
5. Li, Y. & Gu, H. Relationship between middle stratiform clouds and largescale circulation over Eastern China. *Geophys. Res. Lett.* **33** (9), L09706 (2006).
6. Patnaude, R., Diao, M., Liu, X. & Chu, S. Effects of thermodynamics, dynamics and aerosols on cirrus clouds based on in situ observations and NCAR CAM6. *Atmos. Chem. Phys.* **21** (3), 1835–1859 (2021).
7. Cai, H., Yang, Y. & Chen, Q. Distribution characteristics of cloud types and cloud phases over China and their relationship with cloud temperature. *Remote Sens.* **14** (21), 5601 (2022).
8. Zhang, W., Li, J., Xu, S., Zhao, Y. & Jian, B. Spatio-temporal variation of critical relative humidity based on multiple datasets. *Remote Sens.* **15** (17), 4187 (2023).
9. Diao, M. et al. Cloud-scale ice-supersaturated regions spatially correlate with high water vapor heterogeneities. *Atmos. Chem. Phys.* **14** (5), 2639–2656 (2014).
10. D'Alessandro, J. J. et al. Cloud phase and relative humidity distributions over the Southern ocean in Austral summer based on in situ observations and CAM5 simulations. *J. Clim.* **32** (10), 2781–2805 (2019).
11. Schoeberl, M. R. et al. Water vapor, clouds, and saturation in the tropical tropopause layer. *J. Geophys. Res. Atmos.* **124** (7), 3984–4003 (2019).
12. Muhlbauer, A. T. et al. Impact of large-scale dynamics on the microphysical properties of midlatitude cirrus. *J. Geophys. Res. Atmos.* **119** (7), 3976–3996 (2014).
13. Klein, S. A. & Hartmann, D. L. The seasonal cycle of low stratiform clouds. *J. Clim.* **6** (8), 1587–1606 (1993).
14. Wood, R. & Hartmann, D. L. Spatial variability of liquid water path in marine low cloud: the importance of mesoscale cellular convection. *J. Clim.* **19** (9), 1748–1764 (2006).
15. Platt, C. M. R. & Dilley, A. C. Remote sounding of high clouds. IV: observed temperature-variations in cirrus optical-properties. *J. Atmos. Sci.* **38** (5), 1069–1082 (1981).
16. Platt, C. M. R., Scott, S. C. & Dilley, A. C. Remote sounding of high clouds. VI: Optical-properties of midlatitude and tropical cirrus. *J. Atmos. Sci.* **44** (4), 729–747 (1987).
17. Platt, C. M. R. et al. The optical properties of Equatorial cirrus from observations in the ARM pilot radiation observation experiment. *J. Atmos. Sci.* **55** (11), 1977–1996 (1998).
18. Platt, C. M. R. et al. LIRAD observations of tropical cirrus clouds in MCTEX. Part I: optical properties and detection of small particles in cold cirrus. *J. Atmos. Sci.* **59** (22), 3145–3162 (2002).
19. Noel, V., Chepfer, H., Ledanois, G., Delaval, A. & Flamant, P. H. Classification of particle effective shape ratios in cirrus clouds based on the lidar depolarization ratio. *Appl. Opt.* **41** (21), 4245–4257 (2002).
20. Wang, Z., Chi, R., Liu, B. & Zhou, J. Depolarization properties of cirrus clouds from polarization lidar measurements over Hefei in spring. *Chin. Opt. Lett.* **6** (4), 235–237 (2008).
21. Liu, Z. et al. The CALIPSO lidar cloud and aerosol discrimination: version 2 algorithm and initial assessment of performance. *J. Atmos. Ocean. Technol.* **26** (7), 1198–1213 (2009).
22. Zhang, Y., Ren, H. & Pan, X. *Integration Dataset of Tibet Plateau Boundary* (National Tibetan Plateau Data Center, 2019).
23. NOAA NCEI. ETOPO 2022 15 Arc-Second Global Relief Model. NOAA National Centers for Environmental Information. (2022). https://doi.org/10.25921/fd45-gt74. Accessed on 2023-11-25.
24. Krämer, M. C. et al. A microphysics guide to cirrus clouds-Part 1: cirrus types. *Atmos. Chem. Phys.* **16** (5), 3463–3483 (2016).
25. He, Q. et al. The role of ASM on the formation and properties of cirrus clouds over the Tibetan plateau. *Tellus B.* **71**, 1445379 (2019).
26. Wernli, H., Boettcher, M., Joos, H., Miltenberger, A. K. & Spichtinger, P. A trajectory-based classification of ERA-Interim ice clouds in the region of the North Atlantic storm track. *Geophys. Res. Lett.* **43** (12), 6657–6664 (2016).
27. Krämer, M. C. et al. A microphysics guide to cirrus-Part 2: climatologies of clouds and humidity from observations. *Atmos. Chem. Phys.* **20** (21), 12569–12608 (2020).
28. Alexei, K. & George, A. I. Relative humidity in liquid, mixed-phase, and ice clouds. *J. Atmos. Sci.* **63** (11), 2865–2880 (2006).
29. Zhang, F. et al. Possible mechanisms of summer cirrus clouds over the Tibetan plateau. *Atmos. Chem. Phys.* **20**, 11799–11808 (2020).
30. Tetens, V. & O Uber einige meteorologische begriffe. *Z. Geophys.* **6**, 297–309 (1930).

Acknowledgements

Author contributions

Conceptualization, Y. Y. and H. - K. C.; Methodology, Y. Y. and H. - K. C.; Validation, Y. Y., H. - K. C. and Q. - L. C.; Formal analysis, Y. Y. and H. - K. C.; Investigation, Y. Y. and H. - K. C.; Data curation, Y. Y.; Writing—original draft preparation, Y. Y.; Writing—review and editing, Y. Y. and H. - K. C.; Visualization, Y. Y.; Supervision, Q. - L. C. All authors have read and agreed to the published version of the manuscript.

Declarations

Competing interests
The authors declare no competing interests.

Additional information
Correspondence and requests for materials should be addressed to H.C.

Reprints and permissions information is available at www.nature.com/reprints.

Publisher's note Springer Nature remains neutral with regard to jurisdictional claims in published maps and institutional affiliations.